OXFORD JOURNAL
OF STUDENT
SCHOLARSHIP

Hydrological Revival and Subsequent Contraction of Lake Manly: A Case Study of Extreme Precipitation Events and Their Impact on Endorheic Watersheds in Death Valley, 2023–2024

Tony Mehani | Research conducted under the mentorship of Dr Amanda Schmidt
tonymeha@tasisengland.org

ABSTRACT

Extreme precipitation in 2023–2024 temporarily re-established Lake Manly in Death Valley's endorheic Badwater Basin. This retrospective observational study integrates Landsat 8/9 and Sentinel-2 satellite imagery, USGS 3DEP topography, NOAA precipitation records, and NASA SWOT-derived water-depth estimates to investigate the lake's formation, expansion and contraction. Following Hurricane Hilary on 20 August 2023, mapped lake area reached 31.18 km² in September and declined to approximately 23 km² by late November. Following the atmospheric river event of 4-7 February 2024, the largest sampled area was 43.95 km² on 23 February, with an estimated mean depth of 0.7 m and volume of 30.765 million m³. By 4 March, estimated lake volume had decreased to 15.580 million m³, a 49.4% decline, while surface area fell by 11.4%. This disproportionate storage response highlights the importance of depth in interpreting shallow ephemeral lakes. Although evaporation, infiltration and wind-driven redistribution may contribute to observed changes, the available observations do not quantify their individual effects. The study illustrates the sensitivity of endorheic basins to episodic precipitation and identifies observational constraints on hydrological attribution.

Keywords: *Lake Manly; Badwater Basin; endorheic watershed; atmospheric rivers; Hurricane Hilary; remote sensing; SWOT*

1. INTRODUCTION

1.1 Background

Death Valley is one of the most arid landscapes on the planet (National Park Service, 2024). At the lowest elevation in Death Valley, Badwater Basin can be found (USGS, n.d). It is the endpoint of a closed watershed where water enters through precipitation and surface runoff but has no external surface-water outlet, and may be lost through evaporation, infiltration or ground-water exchange (USGS, n.d). These types of drainage basins are referred to as endorheic watersheds, which essentially means that any water entering the system is stored internally instead of being discharged to the ocean via rivers and streams

(USGS, n.d). Because of the fact that water cannot exit the system or basin via surface outflow, even short term periods of high precipitation levels can cause extreme hydrological changes that wouldn't typically be present in open drainage systems (National Park Service, 2024).

Under typical hydrological conditions, the Basin is a salt flat, yet throughout the duration of the 2023–2024 weather events, this changed (National Park Service, 2024). Unusually intense atmospheric river conditions coupled with the lingering effects of Hurricane Hilary were essential in transforming this dry salt flat into what is known as Lake Manly: a temporary lake that had not been present at such magnitude for years (National Park Service, 2024). Atmospheric rivers are defined as long, narrow atmospheric corridors transporting concentrated water vapour from the Pacific Ocean to the western United States, and they have been responsible for a large proportion of California's precipitation levels (Ralph et al., 2019; Dettinger, 2011). Although they occupy only a small percentage of area in the atmosphere, on a global scale, atmospheric rivers transport over 85% of the earth's atmospheric vapour in the poleward direction (Dettinger, 2011). In the western regions of North America, they provide a large percentage of the annual precipitation, but they rarely move so far as to cause floods within Death Valley, marking the unusual nature of the 2023–2024 weather events (Ralph et al., 2019; National Park Service, 2024).

1.2 Literature Review

Pre-existing studies suggest that atmospheric rivers have a large effect on extreme precipitation events within the Western regions of the United States. In fact, Ralph et al. (2019) constructed a classification scale for atmospheric rivers that distinguishes them based on their respective intensity and duration: allowing us to use a framework to cross reference the atmospheric river that caused the revival of Lake Manly. Dettinger (2011) even went to forecast and suggest that climate change will exacerbate the volume of water vapour transported via these atmospheric rivers and therefore increase flooding incidence, although scholars still stipulate that the frequency of atmospheric rivers is difficult to predict or quantify as of now. Inside Death Valley specifically, the National Park Service (2024) has identified the after-effects of Hurricane Hilary in August of 2023 combined with the arrival of an atmospheric river in mid February of 2024 as the major extreme weather events which caused the revival of Badwater Basin. The NASA Jet Propulsion Laboratory (2024) was able to show how SWOT Water Surface Elevation Measurements combined with land-elevation data that USGS provides could provide approximations for the quantity change in the lake's volume of water over time.

From a broader perspective, the D-infinity flow algorithm developed by Tarboton (1997) with the USGS 3DEP Elevation Data allow us to hydrologically delineate the boundaries of the watershed around the complex terrain of Badwater Basin, whereas Landsat 8 and Sentinel 2 imagery complement this analysis by providing observations of changes in lake surface area.

1.3 Research Gap and Significance

As climate change continues to accelerate, so does the severity and frequency of extreme meteorological events across the globe, and specifically the Western terrain of the United States, but our understanding of the thresholds and quantified hydrologic effects remains limited. Although previous studies have documented the meteorological events associated with Lake Manly's reappearance, the temporal relationship between precipitation, changes in lake surface area, estimated water depth and subsequent contraction remains insufficiently resolved. By integrating optical satellite imagery, SWOT-derived depth estimates and topographic analysis, this study examines how the lake's observable response developed across successive precipitation events, while distinguishing measured changes from hypothesized hydrological mechanisms.

1.4 Research Question and Hypotheses

This study asks: What was the effect of extreme weather events in 2023–2024 on the revival of Lake Manly, and which watershed dynamics can explain its short-lived appearance and disappearance? It tests three observational hypotheses: H1, mapped lake area increases following the 20 August 2023 and 2 February 2024 precipitation episodes; H2, estimated lake volume contracts proportionally faster than mapped surface area between 23 February and 4 March 2024; and H3, the largest observed lake area follows rather than coincides with the 4–7 February atmospheric-river event. These hypotheses can be evaluated against the sampled time series, but their confirmation does not prove that an individual meteorological or water-loss mechanism caused the change.

2. MATERIALS AND METHODS

2.1 Study Design

This research utilised a retrospective, observational design to explore the revival and subsequent disappearance of Lake Manly in Badwater Basin in the time period between 20 August 2023 and April 2024. The study combined remote sensing, topography, and meteorological data to reconstruct changes in the lake's hydrological characteristics following Hurricane Hilary and the 2 February 2024 atmospheric river event. Landsat 8/9 and Sentinel 2 images were used to estimate Lake surface area. NOAA (National Oceanic and Atmospheric Administration) data was used to find the temperature and precipitation data. To delineate the boundaries of the watershed and remodel the topography and drainage pathways of the landscape, USGS 3DEP elevation data was utilised. To examine variations in the surface lake moisture during the expansion and contraction of the lake, NDMI (Normalized Difference Moisture Index) data was used. Together, all these datasets were aligned chronologically on a graph to explore whether the timing of the extreme precipitation events was closely linked to lake surface area, depth, temperature or moisture; with time lags around the hydrological watershed processes being subject to further evaluation.

2.2 Study Area

The study zoomed in on Lake Manly, a temporary lake that appeared at Badwater Basin in Death Valley National Park, California, United States. The centre of the study area was Latitude: 36.215° N, Longitude: −116.770° W, and the delineated study area covered approximately 518 km^2. Badwater Basin is the lowest point of an endorheic watershed, resulting in all surface runoff draining into it to pool, rather than flowing through an outlet to the Pacific Ocean. As a subsequent result, surface runoff and precipitation that reaches the basin pools at the lowest elevations before being lost through evaporation or subsurface infiltration. The study period extended from 1 August 2023 to 30 April 2024. This time period was chosen in order to include lake conditions before the effects of Hurricane Hilary were apparent, re-expansion following the 4-7 February 2024 atmospheric river event, and the later disappearance of the lake once more in April 2024.

2.3 Software and Data Sources

Spatial data processing and GIS analysis were conducted using QGIS. Satellite images were typically accessed through USGS, and the SENTINEL HUB, whereas numerical calculations were carried out using a TI-84 Calculator, and graphs were produced using Google Sheets. The NOAA National Centers for Environmental Information were used to procure meteorological records, whilst topographic data was collected from the USGS 3DEP (3D Elevation Program). NASA's SWOT (Surface Water and Ocean Topography) mission was used to collect water depth datasets. Daily precipitation datasets were collected to graph and identify the sequence of rainfall episodes in Death Valley. Then, mean air temperature datasets were also mapped in order to identify the surrounding environmental conditions for the lake appearing and then vanishing. Because direct measurements of evaporation were unavailable (which would have been a main channel for water to leave the lake), air temperature was used to characterize thermal conditions rather than directly estimate evaporation. Landsat 8/9 and Sentinel-2 images were utilised to visually map the variations in the spatial makeup of Lake Manly. The images available exposed a timeline for the valley; before the flood, during initial lake formation, at the lake maximum, and then its gradual disappearance. USGS 3DEP was essential to delineate the surrounding drainage pathways for Badwater Basin and in doing so, identify clearly the basin topography. NASA SWOT-derived-water surface elevation data were used to map water depth for the following dates: 2 February, 12 February, 23 February and 4 March 2024. Simultaneously, Sentinel-2 NDMI images were evaluated for the following days: 12, 22, and 27 February; 3, 8, 18, 23 and 28 March; and then finally, on the 27th of May 2024.

2.4 Watershed Delineation

Using a USGS 3DEP digital elevation model, and in QGIS, the watershed drainage surrounding Badwater Basin was delineated. The elevation data was selected solely to the region around Death Valley to minimise the computational area while still maintaining the upslope terrain characterizing badwater basin's runoff pooling.

From this digital elevation model, a flow-direction raster was then constructed to expose the direction and elevation at which water is predicted to flow. Then, the accumulation of water was quantified to identify outstanding locations for runoff pooling due to considerably steep surrounding cells. Then, the cells with

the greatest accumulated flow were selected as potential drainage paths. Afterwards, Badwater Basin was identified as the terminal collection point due to its position as the lowest point of the watershed. The upslope cells contributing flow toward the selected outlet point were identified and used to delineate the watershed boundary. Moreover, when the resultant boundary was evaluated with the neighbouring relief, the hillshade layers and drainage pathways, we were able to analyse the delineation model with the real topographic structure of Death Valley and ensure its accuracy. This watershed topographical analysis was used to elucidate the reasons why surface runoff typically converged within Badwater Basin rather than neighbouring channels.

2.5 Satellite Image Selection and Preprocessing

To map the main stages of development of Lake Manly between 20 August 2023 and April 2024, Landsat 8/9 and Sentinel 2 images and observations were chosen and used. The main stages of the developmental cycle were pre-flood condition, the appearance of the lake after Hurricane Hilary, the semi-disappearance of the lake, revival of the lake following the 2 February 2024 atmospheric river, and then the final decline of the lake in March-April 2024. Each image was evaluated before being used in the study to examine if the lake and basin were clear enough for comparison; images with significant pieces of cloud obstruction over the case study area (Badwater Basin) were discarded. The selected images were compared using a consistent geographic extent to reduce differences arising from map framing. However, differences in sensor resolution, acquisition conditions and spectral response may still influence the apparent lake boundary. From a comparative perspective, Landsat and Sentinel-2 images are different in terms of the spatial resolution and acquisition timing. Therefore, the image sequence was taken into account more so as an array or a collection of discrete observations instead of a continuous day by day examination of the lake's hydrological condition. Therefore, variations in the lake's hydrology between different satellite images couldn't be pinpointed to a specific day.

2.6 Lake-Surface Delineation and Area Calculation

The visually identifiable boundary of Lake Manly was manually delineated from the selected satellite images. The body of water at the lowest point of Badwater Basin was distinguished or identified from the neighbouring and surrounding hydrological features using different colours. Then, for each selected observation date, a polygon was constructed as closely as possible to the lake boundary. This polygon had an area in square kilometres, and the resulting area readings were collected and laid out chronologically to track the exact changes in the lake's expansion and disappearance between 20 August 2023 and April 2024. Since the boundaries and differences between shallow lake water and exposed salt crust couldn't be clearly delineated or identified, all area readings were used as evidence of a larger trend, rather than exact quantitative data points. To increase consistency and reproducibility between different image dates, similar visualisation criteria were used.

2.7 Precipitation Analysis

Daily precipitation data were obtained from NOAA and arranged in chronological order from 20 August 2023 to late April 2024. Through this, two major periods of extreme precipitation were identified. The first was the rainfall following Hurricane Hilary in August 2023, and the following was the atmospheric

river event of 2 February 2024 that reached all of Death Valley. Both precipitation episodes preceded periods of lake expansion. To examine this temporal association, the timing and magnitude of precipitation were compared with satellite-derived observations of lake surface area. In order to examine whether there was a lag between precipitation and lake changes, the number of days between area changes and precipitation was examined. However, due to the limitation of satellite imagery not being continuously available, the lag identified was more so a quantification of the time interval elapsing between meteorological forcing and the next observable lake response rather than a direct measurement of runoff travel time. This temporal comparison was used to examine whether observed lake changes followed precipitation immediately or after a measurable interval.

2.8 Lake Depth Estimation

Using NASA's analysis of SWOT water surface elevation measurements and USGS ground-elevation data, estimates for the lake depth were found for 2 February, 12 February, 23 February and 4 March 2024. The water depth was specifically quantified using the vertical difference between the water surface level and the elevation of the ground floor water basin.

$$d_i = h_{water,i} - h_{ground,i}$$

where d_i is estimated water depth at location i, $h_{water,i}$ is SWOT-derived water-surface elevation, and $h_{ground,i}$ is USGS-derived ground elevation, all in metres.

Moreover, the NASA depth map represents the spatial distribution of water-depth across Lake Manly at every date chosen. From this mapped distribution for each day, a mean value for depth was estimated and then utilised as characterization of the lake as a whole. It's essential to note that these values were treated as approximations in order to not generalize or over simplify the variation present across the basin topography, but rather to construct a temporal comparison of lake conditions.

2.9 Lake Volume Estimation

Approximations for the volume of water stored in Lake Manly were carried out through the multiplication of the lake surface area and the mean depth (estimated) for each SWOT observation date. The following formula was used:

$$V = A\bar{d}$$

$$1\ km^2 = 1,000,000\ m^2$$

$$V(m^3) = A(km^2) \times 10^6 \times \bar{d}(m)$$

This calculation was used for 2 February, 12 February and 4 March 2024. The limitation of this estimation is that it suggests that the mean depth, which is itself an estimation, is an adequate representation for the entire lake. It doesn't incorporate small variations in basin depth. Therefore, the output values for lake

depth were used as evidence of an overall trend in lake storage rather than exact quantitative values for lake storage. Pixel-level uncertainty estimates were not available online for these mean depth values.

2.10 NDMI Analysis

$$NDMI = \frac{NIR-SWIR}{NIR+SWIR}$$

Where NIR is near-infrared reflectance and SWIR is short-wave infrared reflectance.

Subsequently, the results for lake volume were evaluated from a temporal perspective. Variations in the surface moisture around Badwater Basin were evaluated through the use of the NDMI moisture index from the Sentinel-2 imagery. The NDMI itself is derived from near-infrared and short-wave infrared reflectance.

The NDMI sequence incorporated observations from the 12, 22 and 27 of February; with the sequence being used to analyse whether or not the spatial extent of wet surfaces decreased along with the visual water contraction of the lake itself.

2.11 Air Temperature Analysis

Using mean air temperature records from NOAA, seasonal changes in thermal conditions from August 2023 to April 2024 were compared with the developmental stages of Lake Manly. Moreover, temperature was used as an indicator of potential evaporation, as evaporation is intertwined with solar radiation and surface conditions. Temperature variations were evaluated alongside changes in lake area and volume to examine whether the lake's disappearance or contraction coincided with changing thermal conditions.

2.12 Integrated Temporal Analysis

$$x_{norm} = \frac{x-x_{\min}}{x_{\max}-x_{\min}}$$

All the investigated factors – temperature, precipitation, lake surface area, and estimated volume of water within the lake – were all mapped on a chronological timeline to evaluate trends in the timing of lake hydrology variations. Since all of the variables were quantified in different units, all the series were standardized or normalised using minimum and maximum normalization. What normalization achieved was converting different variables into a universal scale from 0 to 1.

Then, the specific time periods containing Hurricane Hilary and the 2 February024 atmospheric river event were marked on the hydrological timeline, allowing all changes in trends to be evaluated side by side with changes in the lake's physical hydrology. The aim of this integrated analysis was to clearly map the developmental chronology through which variables such as precipitation and temperature affect the

lake's expanded and subsequent disappearance. The analysis was focused on the timing and correlation of all changes rather than the specific quantities since SWOT observations were non-continuous.

Furthermore, estimations for the surface area of the lake were made more uncertain because of how shallow water was blending with saturated sediment. Also, the depth and volume data collected also carried a large degree of uncertainty because the mean depth of the lake used in calculations was a blanket estimate that didn't take into account all the spatial variations in basin depth. Air temperature was utilised as an indicator of evapotranspiration since no evaporation quantitative data was available. In parallel, NDMI data signified variations in the moisture content on the lake's surface level but also didn't quantify the moisture in the atmosphere. Overall, this case study design was successful in finding temporal and spatial correlations and links within precipitation, lake growth and then evaporation, however, it was not able to ascertain that anthropogenic climate change was the root cause of the 2023–2024 weather events or a universally applicable threshold (precipitation based) for the activation of endorheic watersheds.

2.13 Processing Provenance and Reproducibility

The original project describes QGIS-based delineation of the lake surface and the USGS 3DEP watershed, cloud-screened Landsat 8/9 and Sentinel-2 images, NOAA observations, and SWOT-based depth mapping. The original submitted manuscript does not record the satellite scene IDs, individual band combinations, GIS coordinate reference system, DEM cell size, QGIS version, cloud-screening threshold, or independent repeat delineations. These missing settings cannot be responsibly reconstructed from the manuscript alone. The available procedures are therefore reported transparently as a descriptive workflow; a fully reproducible pixel-level reconstruction would require the source QGIS project and satellite acquisition metadata.

2.14 Measurement Uncertainty and Water-Balance Framework

$$\frac{\sigma_V}{V} \approx \sqrt{\left(\frac{\sigma_A}{A}\right)^2 + \left(\frac{\sigma_d}{\bar{d}}\right)^2}$$

For approximate storage V = A × d, where A is mapped surface area and d is estimated mean depth. In the reported units, V (million m³) = A (km²) × d (m). Under independent uncertainties, the first-order relative uncertainty would be $\sigma V/V \approx \sqrt{[(\sigma A/A)^2 + (\sigma d/d)^2]}$. However, the original study did not measure σA or σd, and so numerical confidence intervals or error bars cannot be assigned defensibly. Area estimates are sensitive to the visual boundary between shallow water and salt flats, while the mean-depth estimates are rounded to 0.1 m. Accordingly, volumes are presented as calculated approximations, not high-precision physical measurements. The basin-scale water balance over an observation interval is $\Delta V = P \times A + Qin - E \times A - I - Qout$, where P is direct precipitation depth, Qin is surface/subsurface inflow, E is evaporation depth, I is infiltration loss and Qout represents any additional outflow. There is no surface outlet from this endorheic basin, but the other fluxes are not measured comprehensively. Wind-driven redistribution can alter the spatial pattern of water without necessarily removing volume from the basin. Thus, the observed ΔV cannot uniquely identify evaporation or infiltration.

2.15 Methodological Limitations

It is important to note that the temporal resolution of all aspects of this investigation was affected by the intermittence of the cloud-free satellite images and SWOT data. For example, the real, accurate maximum lake area may have fallen in between two satellite images and was therefore not identified. Moreover, variations in the spatial resolution of Landsat, Sentinel-2, USGS 3DEP and SWOT data incorporated an element of uncertainty in the comparison of data via the hydrological model.

3. RESULTS

This section reports the findings only; interpretation is reserved for the Discussion. This section analyses the changes in precipitation, lake surface area, depth, volume estimations, moisture content in air, and air temperature. The hydrological systems responsible for these changes are evaluated in the Discussion section.

3.1 Watershed configuration and meteorological inputs

Analysis using the USGS 3DEP digital elevation data suggested that Badwater Basin is the lowest point of an internal drainage system. More specifically, the elevation layers exposed how runoff in the neighbouring terrain converges near the valley floor, with no outlet to leave it via external surfaces. The delineated drainage pathways thus affirmed that Badwater Basin is the main accumulation point for water from extreme precipitation events.

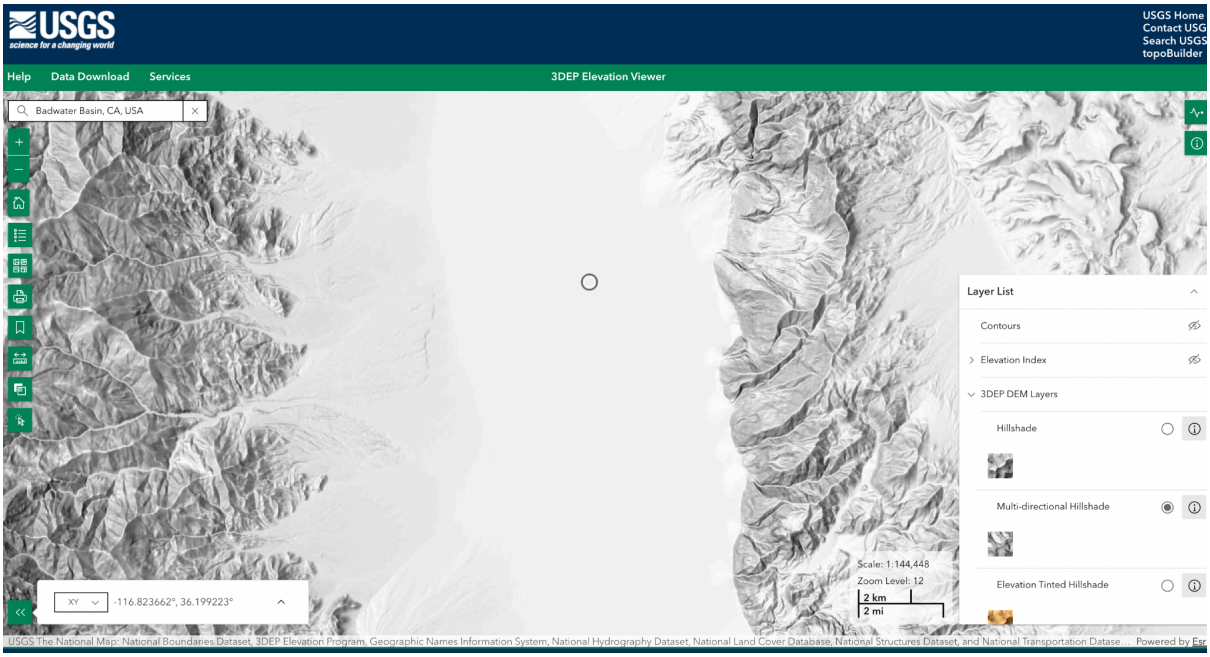


Figure 1 *- USGS 3Dep multidirectional hillshade of Badwater Basin and neighbouring mountainous terrain; exposing basin's steep topography*

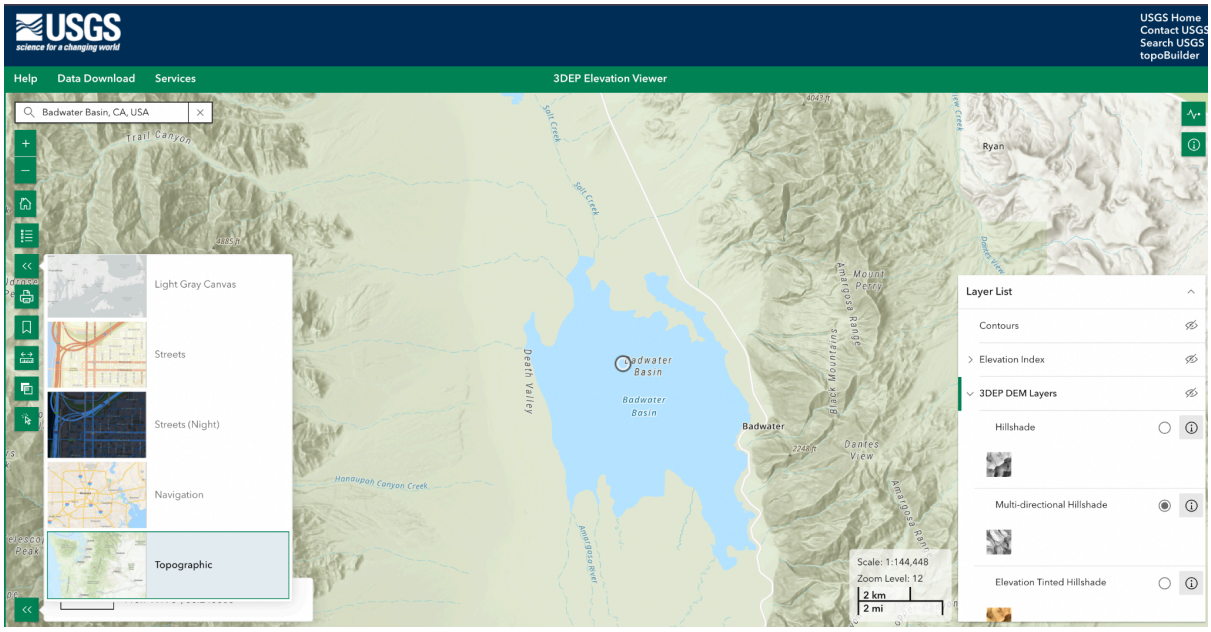


Figure 2: *Topographic mapping of Badwater Basin's water channels*

3.2 Precipitation Data Synthesis

The precipitation dataset exposes two major rainfall periods during the study. The first extreme precipitation event was during the last stages of Hurricane Hilary on the 20th of August 2023. Approximately 55.88 mm of precipitation was calculated at Furnace Creek. The second major precipitation event was during the atmospheric river of early February (4-7) 2024, which resulted in 38.1mm of precipitation. Individually, each of these extreme precipitation events was much greater in scale than the intermediate daily rainfall and comprised the main meteorological inputs that contributed to the appearance of Lake Manly.

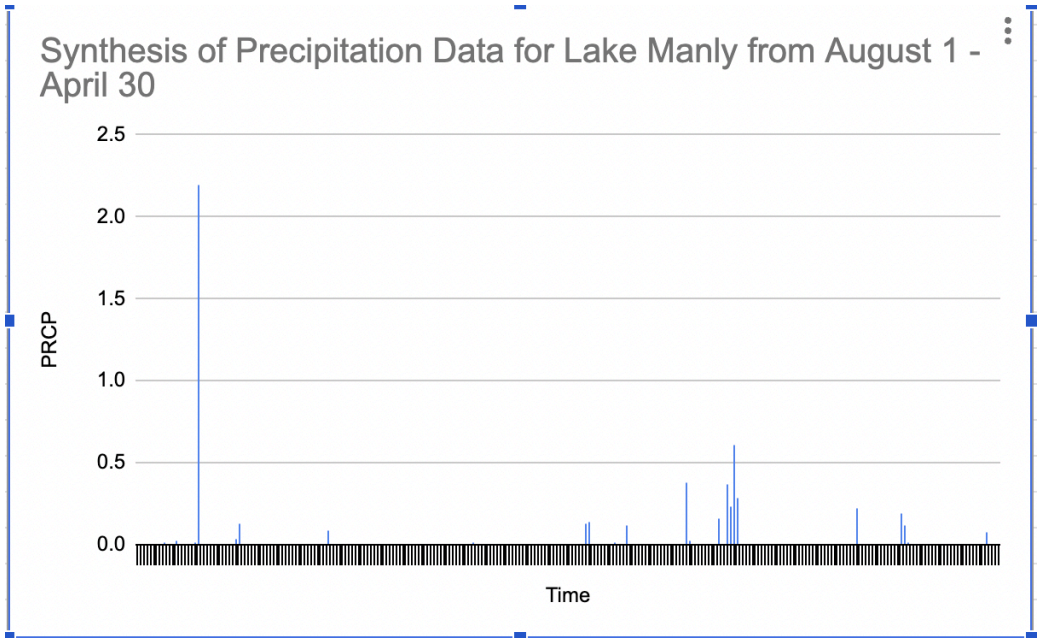


Figure 3: *Synthesis of Daily Precipitation Data (mm) for Lake Manly from August 1 2023-April 30 2024, recorded at Furnace Creek. Data source: NOAA National Centers for Environmental Information*

3.3 Changes in Lake Surface Area

After the August precipitation event, the satellite records picked up on the formation of a large scale body of water at Badwater Basin. Lake surface area began to decrease during late autumn 2023 as less precipitation reached the valley, before increasing again in February 2024 due to the atmospheric river. The intensity of the precipitation events in two short time spans juxtaposed with the lake's existence for many months.

3.3.1 Satellite Imagery Sequence

The sequence of satellite imagery available captured the spatial developmental cycle of Lake Manly from its condition before these extreme weather events through the two phases of appearance and contraction. No lake surface area was captured before Hurricane Hilary, and the water which pooled in the low-lying section of the basin contracted during 2023, expanded during 2 February 2024, and finally shrank in late April 2024.

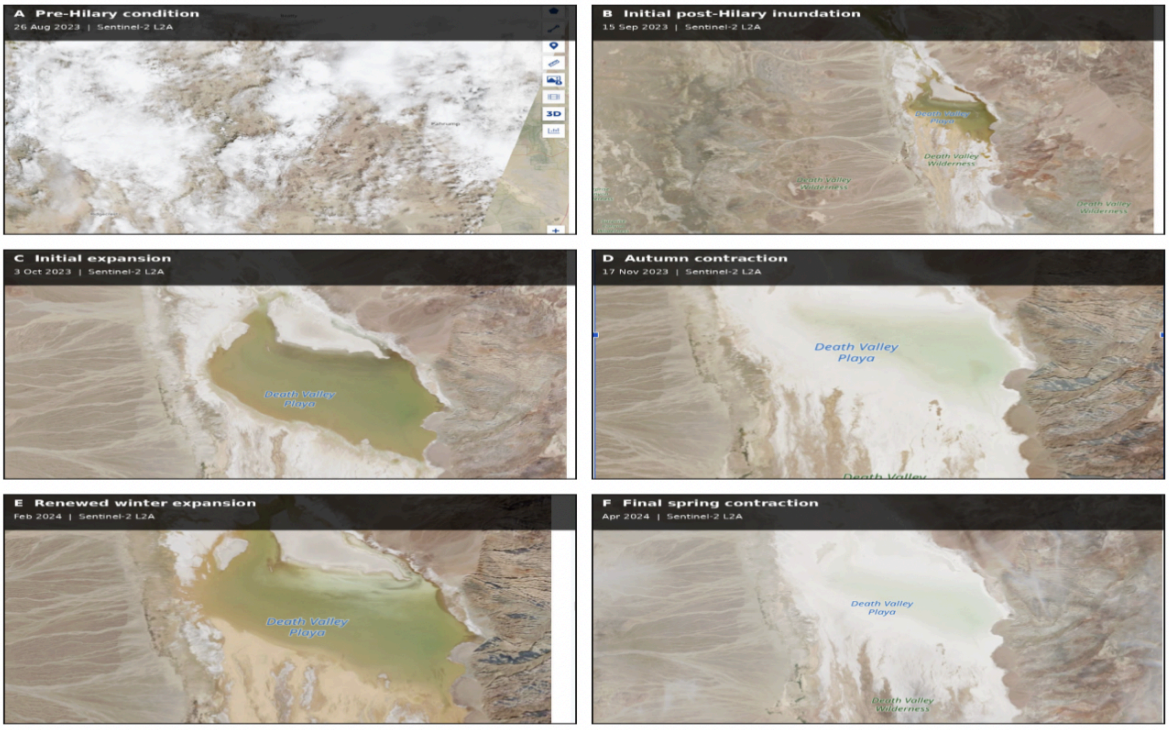


Figure 4. *Satellite imagery sequence exposing the spatial structural changes in Lake Manly from August 2023 to April 2024; (A) lake condition before Hurricane Hilary; (B) initial formation during the aftereffects of Hilary; (C) expansion of lake after; (D) shrinking during autumn 2023; (E) expansion during February 2024 atmospheric river; (F) shrinking during late spring 2024. Landsat 8/9 and Sentinel-2 images were captured using the same boundaries to improve the accuracy of side by side temporal evaluation.*

The sequence of satellite imagery available captured the spatial developmental cycle of Lake Manly from its condition before these extreme weather events through the two phases of appearance and contraction. No lake surface area was captured before Hurricane Hilary, and the water which pooled in the low-lying section of the basin contracted during 2023, expanded during 2 February 2024, and finally shrank in late April 2024.

3.3.2: Lake Surface Area Over Time

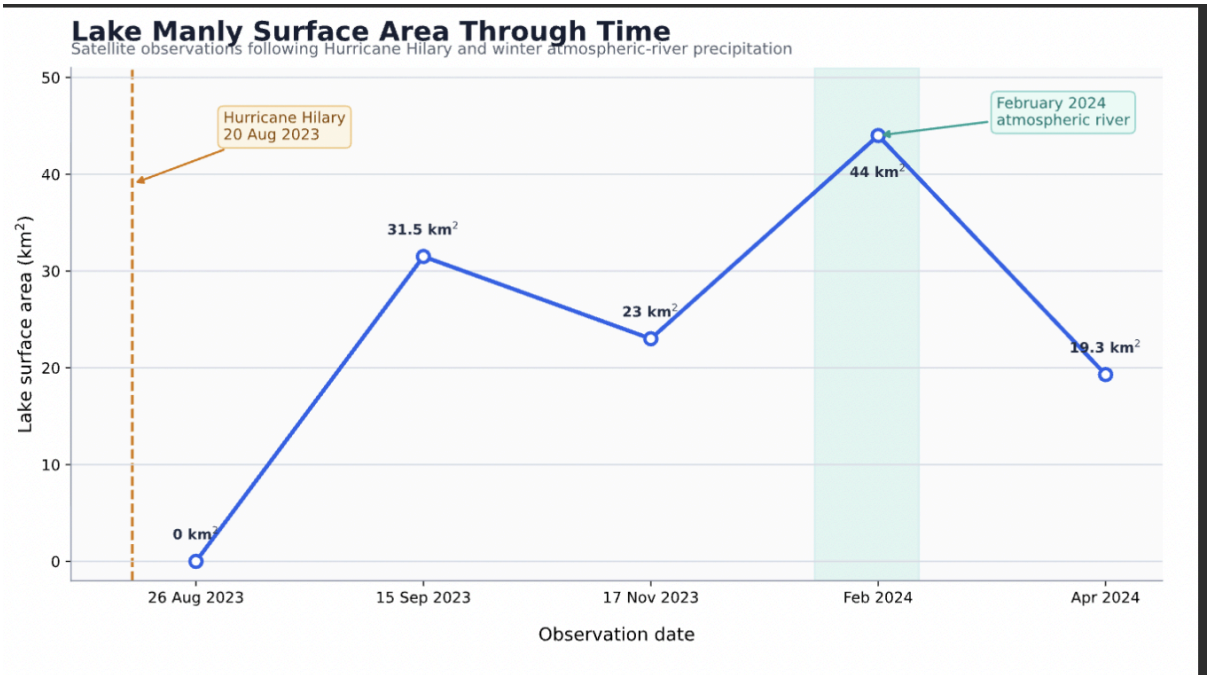


Figure 5: *Continuous Line Graph of Lake Surface Area over Time. Points are extracted from Landsat 8/9 or Sentinel 2 imagery; connecting lines reflect the temporal sequence but do not reflect continuous daily measurements.*

Quantifying the mapped lake boundaries affirmed the structural variations that can be seen in the satellite imagery sequence. In the pre-Hilary August 2023 image no lake surface area was captured, however, after Hilary the lake surface area increased to 31.18 in km September.

By late November, the lake surface area had decreased to 23 km^2. We can see therefore, that despite the decrease in lake surface area, the lake persisted several months after the Hurricane Hilary precipitation in August. Then, from 4-7 February 2024, the lake surface area increased to a peak of 43.95 km^2, amounting to an increase of 41%. $\frac{43.95-31.18}{31.18} \times 100 = 41.0\%$

By late April 2024, the mapped surface area had decreased to approximately 19 km², representing a 56.8% decrease from the February peak. Thus, the surface-area record revealed two periods of lake expansion and contraction associated with the August and February precipitation episodes, separated by a period of reduced lake surface area.

3.4 Lake depth and approximate storage

3.4.1 Lake Depth Mapping

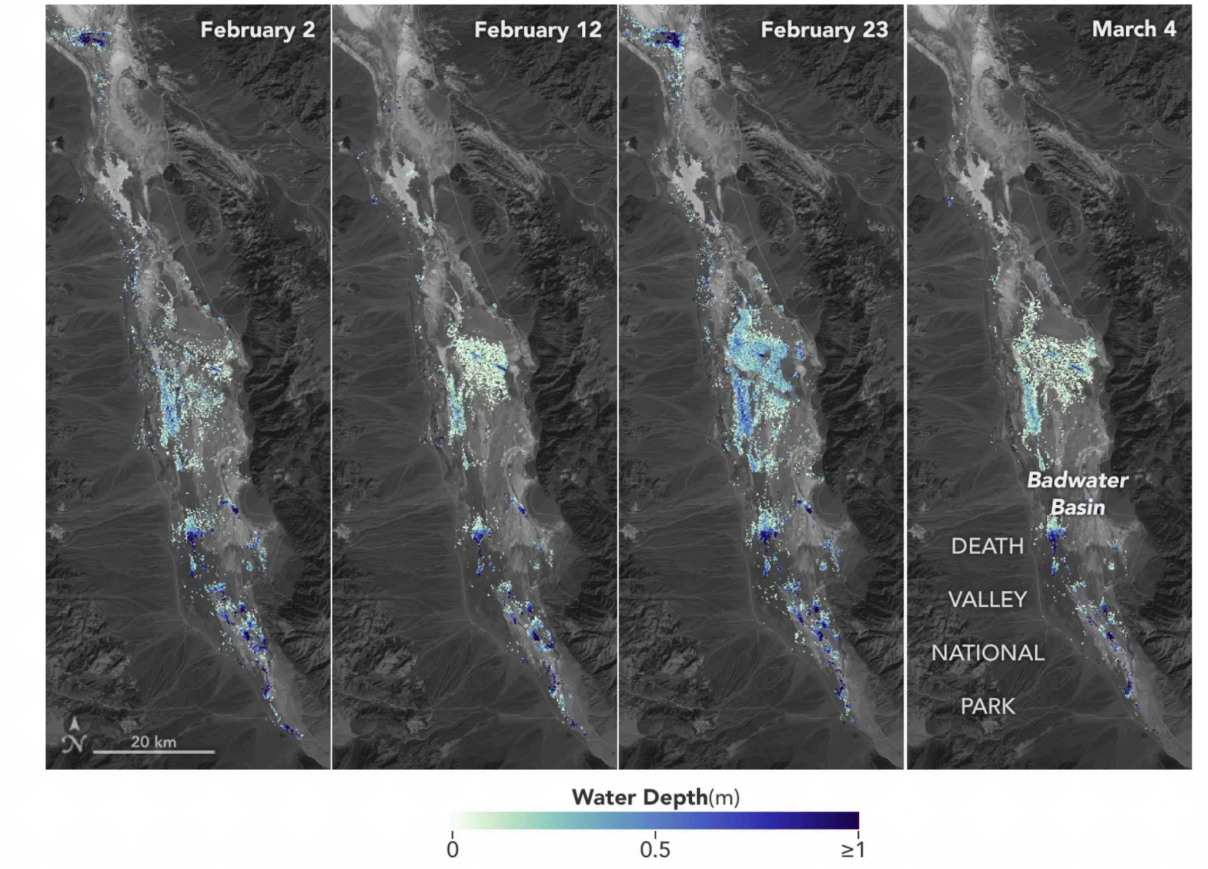


Figure 6: *Sourced from NASA Earth Observatory, made from USGS and SWOT Water Surface Elevation data.*

This SWOT-derived lake sequence exposed variations in the spatial distribution and water depth of Lake Manly between the 2nd of February to the 4th of March 2024. The estimated mean lake depth increased from 0.2m on the 2nd of February to a maximum of 0.7m on the 23rd of February, steadily decreasing to 0.4m on the 4th of March. Data. Estimated spatial distribution and lake depth of Lake Manly between 2 February and 4 March 2024, created through the process of removing USGS basin elevation data from SWOT From 2 to 23 February, the approximate increase in mean lake depth is: $\frac{0.7-0,2}{0.2} \times 100 = 250\%$. Then, from 23 February to 4 March, it decreased by: $\frac{0.7-0.4}{0.4} \times 100 = 42.9\%$.

Meanwhile, the lake surface area increased from 31.18 km^2 on 2 February to 37.82 km^2 on 12 February and then a peak of 43.95 km^2 on 23 February. It also decreased to 38.95 km^2 by the 4th of March. This shows a parallel between lake surface area and mean depth.

3.4.2 - Estimated Lake Volume

The following table presents approximate lake volumes calculated using surface area and estimated mean depth.

Table 1: Table of Estimated Surface Area, Mean Depth and Approximate Volume of Lake Manly from 2 February to 4 March 2024

Date	Area (km^2)	Estimated mean depth (m)	Approximate volume (million m^3)
February 2	31.18	0.2	6.236
February 12	37.82	0.3	11.346
February 23	43.95	0.7	30.765
March 4	38.95	0.4	15.58

3.4.3. Lake Volume Over Time

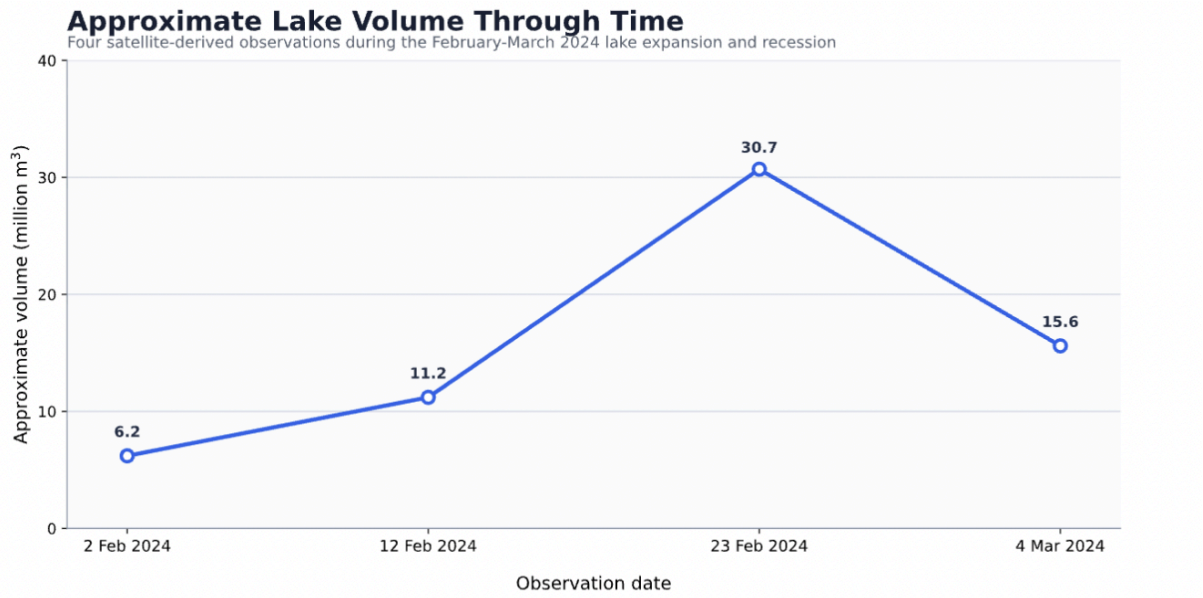


Figure 7: *Graph of Approximate Volume Over Time between 2 February and March 4 2024. Volume was estimated by calculating mapped surface area and approximating mean depth and multiplying together. Once more, points are representative of discrete observations rather than continuous daily measurements.*

The estimated approximate lake volume aligned with the same trend as surface area but there was a greater percentage change or proportional variation because both the surface area of the lake and the mean depth increased. Specifically, volume increased from approximately 6.236 million m³ on 2 February to 11.346 million m³ on 12 February, reaching its maximum of 30.765 million m³ on 23 February. $\frac{30.765-6.236}{6.236} \times 100 = 393.3\%$. By 4 March, the estimated lake volume decreased further.

Although the surface area of Lake Manly decreased by only 11.4% from 23 February to 4 March ($\frac{43.95-38.95}{43.95} \times 100 = 11.4\%$) the estimated volume decreased by 49.4%; $\frac{30.765-15.580}{30.765} \times 100 = 49.4\%$. The disparity and difference elucidates the wider trend that decreased in estimated mean depth were much proportionately larger than decreases in lake surface area.

3.5 - Temporal Response to February Atmospheric River

Comparing the precipitation and lake response records for Lake Manly exposed a time lag between the February atmospheric river precipitation and the peak lake measurements. The atmospheric river vanished on 7 2 February 2024, however, the first subsequent SWOT image, taken on 12 February did not show the largest observed value for lake statistics. On the 12 February, the lake area was 37.82 , with a mean depth of 0.3m and an estimated lake km volume of 11.346 million while the maximum lake size wasn't reached until the 23 February, with area being 43.95 , estimated mean depth was 0.7m, and approximations km for volume reached 30.765 million . m

Therefore, we can conclude that the largest response took a lag of 16 days to occur after the atmospheric river's precipitation ended. Since observations for the lake surface area were only taken on specific discrete dates, the value of 16 days is more efficient in determining a delay to the largest hypothetical measurement, instead of the real life hydrological lag.

3.6 Variations in Surface Moisture

The NDMI sequence of images used exposed substantial amounts of surface level moisture around Badwater Basin from late February 2024 to early March: aligning with the time period in which the lake accumulated the largest amount of water (highest surface area, mean depths, and estimated volume)

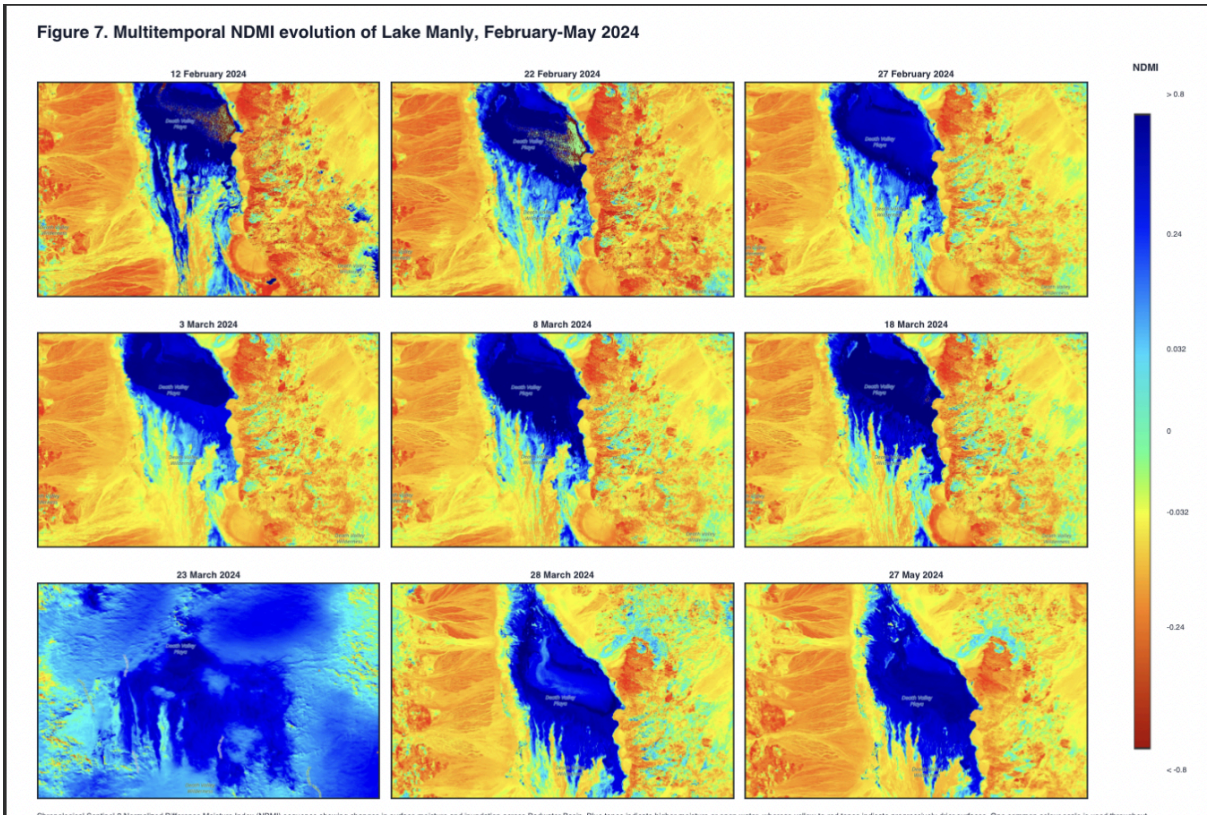


Figure 8. *NDMI sequence exposing variations in surface moisture levels around Badwater Basin from 12 February to 27 May 2024. Higher NDMI values are reflective of a stronger moisture signal however have no correlation with lake depth.*

Table 2. Lake area, approximate mean depth and calculated storage at four sampled dates. Derived storage values retain arithmetic digits for comparison but are not independently validated to three decimal places.

Source: original manuscript's NASA SWOT/USGS interpretation and satellite delineation.

Date	Area (km²)	Mean depth (m)	Volume (million m³)
2 February 2024	31.18	0.2	6.236
12 February 2024	37.82	0.3	11.346
23 February 2024	43.95	0.7	30.765
4 March 2024	38.95	0.4	15.580

The later images taken in March expose a consistent decrease in the spatial extent of the strongest moisture signal. By 27 May, the area of high moisture was much smaller than in February. Although the NDMI values don't reflect a specific measurement of total lake water volume, the sequence itself parallels that of the observed lake contraction.

3.7 - Air-Temperature Over Time

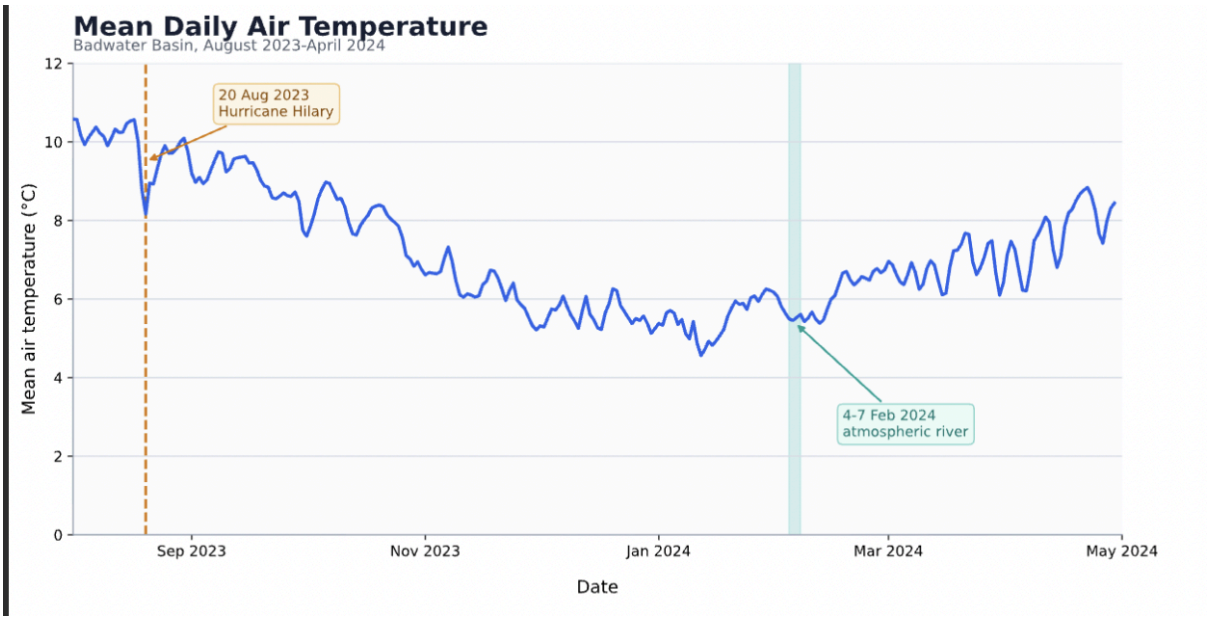


Figure 9: *Mean daily air temperature around Death Valley from August 2023 to April 2024.*

The mean air temperature around Badwater Basin decreased from around 10 °C in August 2023 to approximately 5 °C in January of 2024, as shown in the below figure. Temperatures began to increase from February to April 2024.

The temperature variations were used here to expose or identify larger trends in thermal conditions and evaporation rates, rather than a direct trend. The February lake expansion fell in the colder section of the annual temperature cycle, whilst the subsequent contraction also coincided with increasing temperatures

in spring. Although temperature can't be used to quantify evaporation because other factors such as wind speed need to be considered, the overall upwards trend in temperature increase does solidify the idea of increasing thermal weather during the disappearance of the lake.

3.8 Integrated Hydrological Timeline

Integrating the meteorological and remotely sensed data created an aligned consistent chronological timeline. The first extreme precipitation event of Hurricane Hilary was followed by the formation of Lake Manly only weeks later in September 2023. After that, the contraction of the lake through late autumn and into early 2024, followed by the second major precipitation event of the atmospheric river from 4-7 February which then caused the surface area, approximate lake volume, man air temperature, and

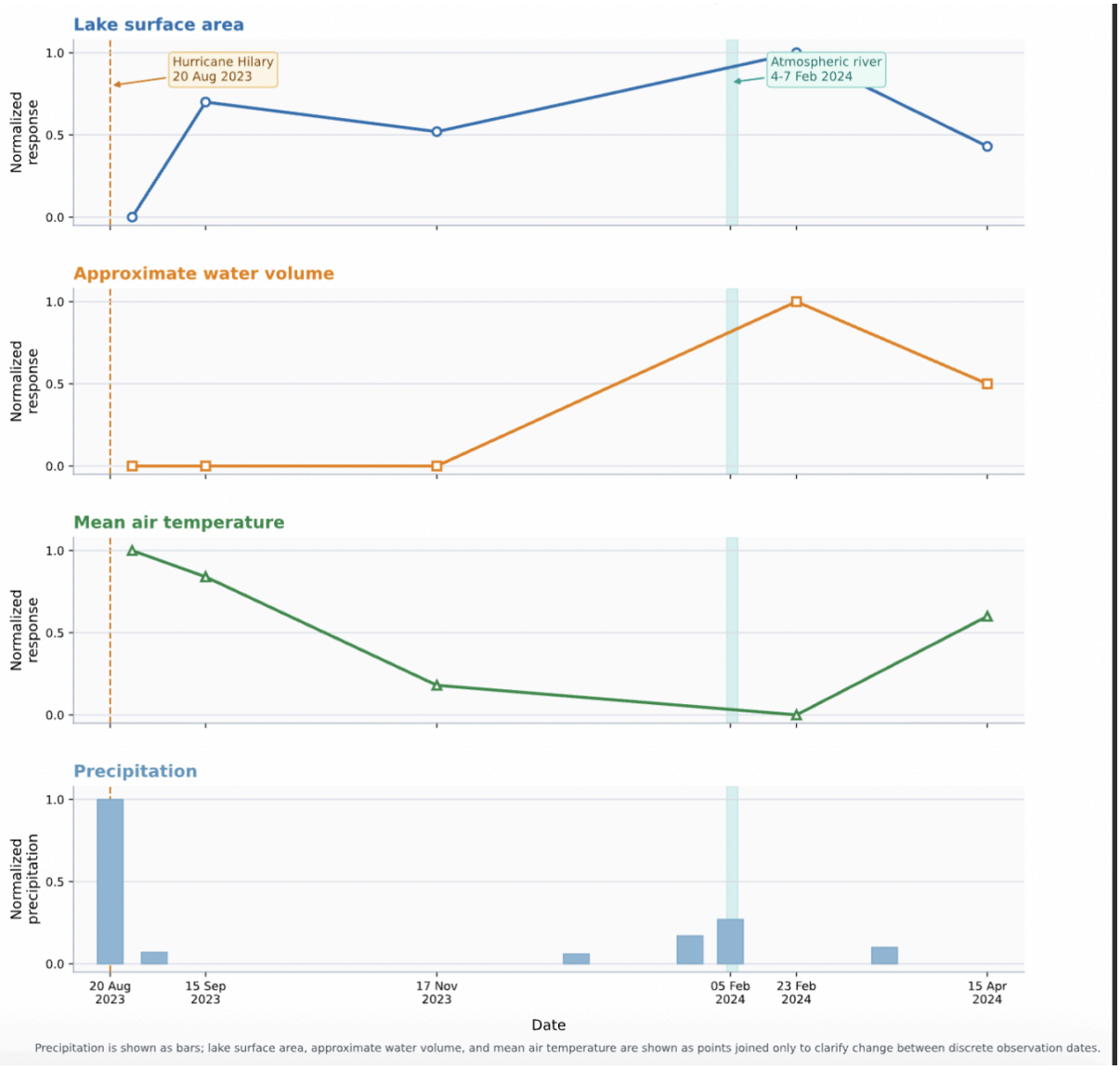


Figure 10. *Integrated hydrological timeline comparing side by side the normalized lake surface area, approximate lake volume, man air temperature, and precipitation in between August 2023 and April 2024. Each variable was normalized on a scale of 0 to 1. Lines are used to link discrete observations and are not representative of continuous measurements.*

precipitation in between August 2023 and April 2024. Each variable was normalized on a scale of 0 to 1. Lines are used to link discrete observations and are not representative of continuous measurements.
The maximum observed surface area, mean lake depth, and approximated volume were recorded on 23 February, only 16 days after the end of the February 4-7 atmospheric river. After this, the variables began to steadily decrease, whilst NDMI moisture imagery exposed a decrease in surface moisture level. Temperature, on the other hand, exposed increasing thermal conditions. Lake volume had a more steep decrease than variables such as surface area, suggesting that the lake became much more shallow before the actual surface water.

3.9 Comparison of Event Timing, Runoff Information and Lake Response

The original NOAA series reports approximately 55.88 mm at Furnace Creek during the August 2023 episode and 38.1 mm for the early 2 February 2024 event. The first figure is associated with 20 August; the source manuscript does not establish consistently whether the second represents a daily observation or accumulated event total. The dates and station basis should be checked against the original NOAA download. The lake area observations indicate expansion following each event, but no contemporaneous discharge series or measured runoff volume is available. The interval between the end of the 4–7 February event and the 23 February sampled maximum is 16 days; this is not a measured watershed travel time.
Table 2. Dated observational sequence: August 2023 precipitation at Furnace Creek (55.88 mm reported); September mapped area 31.18 km²; late November mapped area approximately 23 km²; 4–7 February 2024 precipitation (38.1 mm reported); 2 February area 31.18 km², depth 0.2 m; 12 February area 37.82 km², depth 0.3 m; 23 February area 43.95 km², depth 0.7 m; 4 March area 38.95 km², depth 0.4 m; late April mapped area approximately 19 km². Runoff discharge was not measured, and the observations do not represent a continuous time series.

4. DISCUSSION

4.1 Hydrological Revival Following Hurricane Hilary

The results suggest that Hurricane Hilary set off the first phase of Lake Manly's 2023–2024 appearance or revival. The 55.88 mm of rainfall which was noted at Furnace Creek on 20 August 2023 were far greater than Death Valley's conventional yearly precipitation rates and resulted in large amounts of rapid surface runoff. This was due to the characterization of the surrounding terrain with limited external drainage, steep relief, and sparse vegetation. Moreover, the appearance thereafter of around 31.18 km² of surface water elucidates that the precipitation was magnanimous enough in size to bypass initial infiltration and surface-storage decreases in volume; eventually allowing the accumulation of substantial amounts of

water. However, the formation of Lake Manly can't be attributed entirely to pooling of precipitation at the bottom of the basin. Badwater Basin is the lowest elevation point inside the watershed. The topographic convergence here which was identified through the evaluation and analysis of watersheds thus served to exacerbate the effect of the precipitation. Rainfall distributed across a large area was eventually concentrated inside a comparatively small area. The endorheic structure of this watershed was also a defining feature for why Lake Manly persisted over several months. In a conventional watershed much of the precipitation from the storms would have been output via river discharge into an ocean or sea, however, at Badwater Basin the lack of an external water outlet forced the surface runoff to accumulate and pool inside the basin. This topological feature is responsible for why despite the shortness of the precipitation events. Nevertheless, it is imperative to note that the decrease in lake surface area from 31.18 km² in September to around 23 km² in November suggests that after Hurricane Hilary, the water balance decreased. This is because, after the storm ended, despite the water accumulating at Badwater Basin, losses began to exceed input. Some plausible hydrological mechanisms for this loss are sub-surface infiltration and evaporation, however, the available data doesn't allow a proportion or ratio quantification between them to occur. The existence of a smaller Lake Manly throughout the winter months suggests that the cooler thermal conditions reduced the rate of evaporation enough for some of the initial floodwater to remain there throughout the winter.

4.2 Renewed Revival Following February Atmospheric River

The atmospheric river of 4-7 February 2024 was responsible for around 38.1 mm of precipitation to Badwater Basin. It is important to note that despite the precipitation here being less than the initial precipitation linked with Hurricane Hilary, its deposition whilst residual surface area water from the earlier event was there exacerbated its effects. Therefore, the February atmospheric river added to a hydrological system that hadn't completely dried. After the end of the atmospheric river, the lake surface area steadily increased to 37.82 km² by 12 February and then peaked at 43.95 km² by 23 February. Approximations for the lake's volume also increased from 6.236 million m³ on 2 February up to 30.765 million m³ on 23 February, reflecting a 393.3% spike. The parallel increase in both these variables – lake surface area and volume of water – suggests that the atmospheric river's effects extended beyond distributing the water more widely across the terrain; adding a substantial amount of water. However, an interesting observation is that despite the August rainfall being deeper than that of the February atmospheric river, the February surface area maximum was 41.0% larger than the September measurement. This suggests that rather than solely preserving the previous lake, the atmospheric river resulted in the formation of another phase of inundation. An explanation for this is the continuous impact of antecedent conditions in the lake. For example, residual water, saturated, or even semi-saturated mud sediment decreased the threshold needed for new precipitation to restart accumulation of water. However, because antecedent soil moisture data wasn't available, this is an evidence-based interpretation rather than a directly verified conclusion.

4.3 Lag Between Precipitation and Observed Maximum

The maximum lake area, depth and volume were noted on 23 February; 16 full days following the ending of the atmospheric river. The delay in timing implies that the developmental stages in Lake Manly weren't

instantaneously affected by peak rainfall. This is because the surface runoff across the wider watershed took time to travel through channels before pooling in Badwater Basin. It's also plausible that temporary storage elsewhere could have been a defining factor of this delay. Water sources can be stored briefly inside different pathways before accumulating on the basin floor. Moreover, the low steepness gradient of the playa would also result in slow spreading of the water when entering Badwater Basin. Together, these hydrological processes resulted in a delay even after the end of precipitation.

However, it's important to note that this 16 day interval is not an exact representation of the travel time it took the runoff to reach the lake. This is because SWOT data is taken at ten day intervals; therefore, the stages in lake development were not continuously tracked. The lake itself had begun to increase in size by 12 February, five days after the end of the atmospheric river storm. The hydrological response thus started before this peak. However, the available data limits us from identifying the exact day on which the maximum lake size occurred. Therefore, parts of the lag may be related to sampling frequency rather than an actual delay in hydrological processes. A higher frequency sequence of optical satellite observations is necessary to identify the exact lag time in water accumulation.

4.4 Topographic Control of Lake Formation

Analysis in the watershed topography explains the reason why such short lived precipitation episodes resulted in the creation of such a large lake. Badwater Basin lying under the surrounding terrain, combined with the absence of an external river outlet resulted in flow-accumulation all being directed to the same low elevation point. The geometry of this basin is responsible for the non-linearity of the hydrological response. For example, small precipitation events could be mitigated or absorbed via infiltration or evapotranspiration, however, once the added precipitation exceeds the loss the runoff will begin to accumulate. Moreover, a relatively small increase in precipitation may result in a disproportionately large increase in lake surface area.

The observations from 2023–2024 reflected threshold-like precipitation behaviour, however, they do not permit us to identify a specific universal numeric threshold for the activation of an endorheic watershed. Moreover, only two extreme weather events were analysed, and it's also important to note that precipitation recorded at Furnace Creek doesn't necessarily reflect the wider spatial distribution of rainfall across the entire watershed. Subsequently, we can deduce that the results suggest that both events resulted in water inputs exceeding water outputs in the system, however, they don't allow us to find a single universal precipitation threshold.

4.5 Lake Contraction and Water-Loss Processes

Following 23 February, the surface area of the lake decreased by 11.4%, whilst the estimated lake volume decreased by 49.4% by 4 March. The larger proportional decrease in volume suggests that the lake's structure became shallower more quickly than its visible footprint decreased. This is expected because of the broad, low-gradient nature of the basin: a significant decrease in lake depth can occur whilst the water itself maintains a large surface area. Furthermore, the timing of the water loss was also heavily impacted

by the strong winds from 29 February and 2 March. As per the National Park Service, the winds moved the lake around two miles north and then distributed the water across a larger yet shallower area.

4.6 Relationship Between Surface Area and Volume

The redistribution of lake water also limits the ability to compare between surface area measurements and lake water storage since here, an increase in the visibility of lake surface area doesn't necessarily correlate with an increase in lake volume of water. Wind-driven spreading of the lake could actually increase lake surface area while decreasing its mean depth.

The shallow geometry of the lake would also increase the evaporation rate because of the increased surface area to volume ratio of the water. Moreover, once the influx of water via precipitation decreased, the evaporation of water would result in a decrease in water storage without the need for external surface outflow. Furthermore, increasing spring temperatures paralleled increased evaporation demand during the time period through which the lake contracted, while the NDMI moisture sequence exposed a parallel decrease in surface moisture. Nonetheless, this study was limited by unavailable data for evaporation, infiltration, humidity, solar radiation, or wind speed directly. Thus, temperature and NDMI data are important in contributing contextual information for evaporation rates yet are limited in that they cannot accurately quantify or reveal the proportion of water lost via evaporation or sub surface infiltration. Perhaps, the most plausible conclusion is that the lake contraction was due to the combined water losses from infiltration, wind-redistribution, and evaporation. The results suggest that lake surface area by itself was not sufficient in indicating hydrological water storage. Between 23 February and 4 March, surface area decreased from 43.95 to 38.95 km^2, while the estimated lake volume decreased from 30.765 to 15.580 million m^3. The reduction in surface area was comparatively limited compared to the loss of water volume. This difference was mainly caused by the reduction in estimated mean depth from 0.7 to 0.4 m. In the shallow basin, a small vertical decrease in mean depth would have a corresponding disproportionately large decrease in volumetric quantities held by the water. Combining SWOT analysis with optical satellite imagery was therefore essential in deciphering these datasets together. The optical satellite imagery was relevant in exposing the parts where water was concentrated, whilst mean depth allowed us to explore how much water was stored in the lake. A limitation of the calculation used for lake volume is that it uses only one mean depth for each observation date, however, one mean depth for the lake limits the spatial variability in basin geometry and these depth values used for the mean were procured from remote sensing rather than real, human direct field measurements and data. Thus, the resulting volume output should be analysed in the context of a trend of relative change rather than exact measurements. The data is aligned with pre-existent research that solidifies how atmospheric rivers have disproportionately magnanimous effects in the western regions of the United States. The atmospheric river of February 4-7 2024 resulted in the renewed revival of Lake Manly – increasing its surface area, mean depth, and approximate volume. This revealed that atmospheric rivers can intensify or revive hydrological features even inside a conventionally arid region. Furthermore, the study also aligns with NASA's suggestion of incorporating SWOT data with USGS elevation data to remodel and reconstruct variations in the depth of temporary lakes. Furthermore, the approximate spacing out of the SWOT data in ten day intervals revealed a large increase followed by a quick decrease in the storage of water in the lake;

revealing the value of satellite altimetry in locations such as Badwater Basin where conventional permanent water-monitoring systems aren't present.

4.8 Relationship to Previous Research

The DEM analysis aligned with the theory of Tarboton's flow direction methodology; topographic slopes and contributing areas can be geographically utilised in order to delineate drainage pathways even in the absence of conventional continuous flow rivers or streams. In this exploration, these pathways facilitated the spatial reasoning for the way in which runoff that was initially spread across the terrain eventually concentrated at Badwater Basin. Moreover, the results align with climate-change theories and predictions that hotter temperatures intensify evaporation interlinked with many extreme precipitation events. However, a limitation of this research paper is that it did not extend to formal climate-event causation and attribution; subsequently, determining and identifying that anthropogenic climate change was the root cause of Hurricane Hilary, the atmospheric river and the subsequent reappearance of Lake Manly isn't possible.

4.9 Limitations and Generalizability

The main limitation of this research was the temporal intervals and spacing that the remote-sensing observations resulted in. The satellite imagery and SWOT datasets weren't able to encapsulate a continuous daily record; resulting in uncertainty around the exact date or value for the maximum lake area, depth and volume as it could have fallen between image dates. The calculated 16-day gap following the end of the atmospheric river and the maximum on 23 February is thus indicative of an observational time interval, rather than an exact measurement of hydrological response time.

The surface area estimates were also limited in the difficulty and uncertainty surrounding how to distinguish between shallow water and surrounding hydrological landmarks; saturated sediment, wet salt crust, and more. This could have resulted in either an underestimation or overestimation of the lake delineation boundaries, introducing uncertainty with regards to the lake surface area that would also be carried over into the calculations for total lake volume. Furthermore, variations between the spatial resolution of the two satellites – Landsat and Sentinel-2 – resulted in further uncertainty when comparing side by side the observations. Furthermore, because a single estimated mean depth was used to generalise the entire lake's depth, volume estimates encapsulated another layer of uncertainty. However, it was necessary to output a mean value for depth because of so many variations in the physiology of the terrain. Thus, the mean depth and volume are more relevant as markers of the overall trend through time rather than specific accurate values for quantity.

The NOAA record exposed the precipitation conditions at Furnace Creek rather than quantifying the total rainfall across the whole watershed. Variations in orography could have resulted in differences between the rainfall in surrounding mountains and that recorded at Furnace Creek station. Thus, the meteorological data is more successful in exposing an overall temporal storm strength and intensity relationship rather than encapsulating the total rainfall across the watershed. Moreover, evaporation and filtration were not quantified or measured directly. This created a limitation where temperature and NDMI datasets were

used to suggest trends that would have been more aptly encapsulated through evaporation and sub-surface filtration data. In the future, research could focus on the use of high-frequency radar imagery, and measured quantities for evaporation to ensure a more accurate water balance.

4.10 Wider Implications

Lake Manly is relevant in exposing how even dry, arid endorheic watersheds which have been inactive for extended periods of time can respond sensitively to concentrated precipitation. The behaviour of each endorheic watershed is dependent not only on total rainfall but also on antecedent conditions, watershed area, and topography.

This event is also important in exposing the unreliability of taking surface area as a quantification for lake magnitude. As seen above, shallow lakes can maintain large surface areas despite large losses in water volume. Thus, monitoring systems for bodies of water must incorporate optical imagery, and water surface elevation data. Finally, despite this investigation focusing solely on the events at Badwater Basin, as extreme precipitation events become more common, understanding the way in which dry landscapes interact with extreme precipitation events will be increasingly vital.

Between 23 February and 4 March, calculated storage declined from 30.765 to 15.580 million m^3, a net change of −15.185 million m^3 over ten days, and −1.5185 million m^3 day^{-1} as an interval-average net storage change. This is not an observed evaporation rate: precipitation, surface inflow, groundwater exchange, infiltration, and evaporation are not jointly constrained. Wind-driven redistribution can alter shoreline extent and locally measured depth but is not itself a basin-scale sink. Therefore, the reviewer's requested numerical partition into evaporation, infiltration and wind effects is not identifiable from the underlying observations, and assigning percentages would be speculative.

Interpretation is limited by gaps between cloud-free satellite images and SWOT overpasses; inconsistent spatial resolutions and acquisition times among Landsat, Sentinel-2, SWOT and USGS products; subjective lake-boundary identification where shallow water resembles saturated salt; coarse, rounded mean-depth estimates; a meteorological station that may not represent the entire contributing catchment; missing measured runoff; and absent direct evaporation, infiltration, groundwater and wind-driven displacement measurements. The true maximum may have occurred between image dates. The observed event sequence in one basin does not establish a universal activation threshold, forecast future atmospheric-river frequency, or attribute the individual storms to anthropogenic climate change.

5. CONCLUSION

This research paper explored the impact of the 2023–2024 extreme weather events on the reconstruction and revival of the inactive salt flat of Badwater Basin into the active Lake Manly; focusing on the hydrological watershed dynamics interlinked with, first, its appearance, then its evaporation. The data suggests that the remnants of Hurricane Hilary were what caused the first phase of the lake; with 55.88

mm of rainfall reaching Furnace Creek on 20 August 2023. The lake surface area increased to approximately 31.18 km² by September. Then after shrinking to a surface area of around 23 km² in late November, the lake began to grow once more after the 4-7 February 2024 atmospheric river, which contributed 38.1 mm of precipitation. The greatest maximum response happened on 23 February when the lake surface area grew to 43.95 km², mean lake depth peaked at 0.7m, and the approximated lake volume was 30.765 million cubic metres. Together, the increase in lake volume represented an increase of 393% from 2 February. Despite this maximum lake value being recorded 16 days after the end of the atmospheric river, the intervals of the satellite images result in uncertainty around the accurate hydrological lag or delay time. Moreover, the lake structural changes and formation were determined by the endorheic nature of the watershed, where most surface runoff eventually pooled in Badwater Basin, with no removal outlets via surface outflow. As a result, the lake was also shallower. This is seen between 23 February and 4 March, when despite the lake volume decreasing by 49.4%, the lake surface area decreased by only 11.4%. The disparity in the proportion of the decrease exposes the inefficiency of relying on surface area alone to quantify water loss. Moreover, high winds that resulted in the re-distribution of water from 29 February to 2 March resulted in lake contraction. Steadily increasing temperatures as the spring came in conjunction with decreasing NDMI values reflected this drying developmental phase, however, it didn't quantify the specific processes for loss; it was impossible to distinguish what water was lost through sub-surface infiltration versus evaporation.

Therefore, overall, these findings confirm the hypothesis that the February atmospheric river intensified the extreme conditions that were caused by the remnants of Hurricane Hilary. On a wider note, they expose the potential of endorheic basins and temporary watersheds to exhibit non-linear responses to linear weather events and statistics based on their unique topography. Finally, despite the study not attributing any of these individual extreme weather events to anthropogenic climate change or quantifying a universal threshold number for activation of inactive watersheds, it is successful in exposing the ways in which GIS, optical satellite imagery, SWOT measurements and meteorological records are successful in reconstructing ephemeral lakes in areas where conventional hydrological monitoring isn't available due to the unexpected nature of the watersheds' existence.

The 2023–2024 Lake Manly sequence supports the observational hypotheses that mapped area increased following the two precipitation episodes, that the sampled February maximum followed the early-February storm, and that estimated storage subsequently declined more rapidly in proportional terms than mapped area. The endorheic topography supports runoff accumulation, but the available data cannot partition lake contraction among evaporation, infiltration and wind-driven redistribution. More frequent observations and direct flux measurements are required to resolve the basin water balance.

6. REFERENCES

1. Copernicus. (n.d.). Copernicus Browser documentation
2. Dettinger, M. D. (2011). Climate change, atmospheric rivers, and floods in

3. European Space Agency. (n.d.). Copernicus Open Access Hub documentation.
4. European Space Agency. (n.d.). Sentinel-2 user handbook.
5. Intergovernmental Panel on Climate Change. (2021). Water cycle changes. In Climate change 2021: The physical science basis (Working Group I contribution to the Sixth Assessment Report, Chapter 8).
6. National Aeronautics and Space Administration. (n.d.). MOD16 evapotranspiration
7. National Oceanic and Atmospheric Administration, National Centers for Environmental Information. (n.d.). Daily climate data.
8. National Park Service. (2024). Lake Manly returns to Death Valley.
9. NASA Jet Propulsion Laboratory. (2024). SWOT satellite helps gauge the depth of Death Valley's temporary lake.
10.PRISM Climate Group. (n.d.). Daily climate data
11.Ralph, F. M., et al. (2019). A scale to characterize the strength and impacts of
12.Schmidt, A. H., Lüdtke, S., & Andermann, C. (2020). Multiple measures of monsoon-controlled water storage in Asia. Earth and Planetary Science Letters, 546,
13.Sentinel Hub. (n.d.). Normalized Difference Moisture Index (NDMI).
14.Tarboton, D. G. (1997). A new method for the determination of flow directions and upslope areas in grid digital elevation models.
15.U.S. Geological Survey. (n.d.). 3D Elevation Program (3DEP) documentation.
16.U.S. Geological Survey. (n.d.). Landsat 8 science users handbook.
17.U.S. Geological Survey, Water Resources Mission Area. (n.d.). Watershed delineation
18.Western Weather and Water Extremes Center. (n.d.). Atmospheric river catalog.
19. Miller, D. M., et al. Geologic Evolution of Death Valley.
20. USGS Water Resources Mission Area. Watershed Delineation Methods.
21. ESA Copernicus Open Access Hub Documentation.
22. Western Weather and Water Extremes Center (CW3E). Atmospheric River Catalog.